

Early Detection of Volumetric Defects Using e-NDE during Friction Stir Welding

Dwight Burford, Enkhsaikhan Boldsaikhan, and Adam Wiley

National Institute for Aviation Research
Wichita State University, Wichita, Kansas, USA

Keywords: Friction Stir Welding, Green Manufacturing, Probability of Detection, Gap Study, Non-Destructive Evaluation, Electronic Non-Destructive Evaluation, e-NDE

Abstract

Friction stir welding (FSW) joint quality has been successfully monitored and evaluated with a new electronic Non-Destructive Evaluation (e-NDE) technique. In the e-NDE approach, the dynamic resultant forces acting on the weld tool are monitored and analyzed for consistency. The feedback forces from the loading on the weld tool are measures of material flow resistance that is induced by the rotational and translational motions of the weld tool. Therefore, measuring these forces during the process provides important information about the stability of the plasticized material flow around the weld tool. In an industry-based round-robin program previously conducted, the probability of detection (POD) capability of the e-NDE approach was found to exceed that of a conventional NDE technique based on radiography (X-ray). The emergence of voids was detected with e-NDE at an earlier stage of formation than was detectable by either standard NDE X-Ray techniques or destructive testing techniques. A systematic study was then undertaken to document the capability of e-NDE in detecting volumetric defects caused by the presence of preexisting gaps (simulating production anomalies) in the joint line. Coupons with both triangular and rectangular gaps were prepared from AA2024-T3 plate stock. The e-NDE technique was successfully used to determine the onset of void formation when present.

Introduction

In joining technologies like friction stir welding (FSW), variations and irregularities in the starting joint geometry or incoming stock can potentially lead to inconsistencies and discrepancies in the final product. Burford [1] examined the effects of plate gap, joint offset, and tensile property variations in fully consolidated welds. He found that a certain amount of offset and plate gap was permissible in a friction stir weld with no deleterious effects on strength and, further, that the standard deviation of the tensile strength of the welds was exceptionally low over the entire length of the weld. Widener et al. [2] looked at holes in the weld path to identify their impact on the mechanical and metallurgical properties of the joint. Accordingly, a pattern of circular holes of increasing diameter from 1.6 mm to 3.2 mm (0.063 inch to 0.125 inch) were machined into workpieces along the butt-joint line before welding. Under axial load control, in all cases the weld tool was observed to be able to close the joint without creating a surface defect; however, the presence of weld discontinuities caused failure to occur in the nugget of all the tensile samples [2].

It is important, therefore, to develop a robust manufacturing process that is capable of producing a fully consolidated joint without being significantly impacted by variations and irregularities of the incoming stock. To meet this objective, an in-process monitoring and control system is being tested and advanced for friction stir welding (FSW) to minimize the occurrence of defects, and thereby promote consistent part quality, when fit-up anomalies are present. A significant element of the approach being taken is the proper selection of process parameters to eliminate instabilities resulting from material or part variations and irregularities.

The new detection, and potentially corrective, system evaluated in this study is based on an electronic Non-Destructive Evaluation (e-NDE) approach [3, 4]. In this approach, the dynamic resultant forces acting on the weld tool are measured and analyzed for consistency [5, 6]. One approach is to measure the feedback forces using pressure transducers installed in either the weld head assembly or the weld tool holder. To be effective, the sampling rate of the transducers must be sufficiently high compared to the spindle frequency. Since the feedback forces taken from the loading on the weld tool are measures of material flow resistance that is induced by the rotational and translational motions of the weld tool, they can deliver important feedback information about the stability of the plasticized material flow around the weld tool.

Conceptualization of the e-NDE Approach [4]

In FSW, the side of the weld tool probe is pressed against the workpiece in a manner similar to that of machining with the side of an end mill. However, unlike end mill machining, in FSW the tool design and process parameters are selected such that the displaced material is captured, reconstituted, and joined back to the original material – as opposed to removing it from the work zone in the form of “chips” as is done in machining. Consequently, there are both similarities as well as dramatic differences in the dynamic response of the respective tools used in end milling and FSW, respectively.

In machining, it is important to clear the cut metal (chips) from the tool at a sufficient rate to prevent clogging of tool features, namely the flutes, etc. In FSW the opposite is true. The features of a FSW tool, such as threads, grooves, etc., are expected to become impacted with metal and thereby maintain a full frontal engagement between the tool and the material of the workpiece. In machining, only the tool cutting edges are expected to be in contact with the material ahead of the cutting front. This full engagement between the FSW tool and workpiece leads to unique dynamic behavior not typically experienced in machining. Notwithstanding the differences in tool engagement with the workpiece, however, the two processes share similar behaviors because of the similarities in which the tools are dynamically loaded (i.e. by side loading caused by advancing a rotating tool through the workpiece).

Advanced control techniques in machining have been investigated for reducing chatter. For example, Zhang and Sims [7] assessed the ability of “piezoelectric active vibration damping” to arrest chaotic tool behavior. To reduce defect formation in FSW associated with chaotic tool motion, Arbogast [8], Boldsaikhan et al. [5], and Jene et al. [9] have studied machine tool-workpiece interactions by monitoring force feedback signals. As these studies demonstrate, in both machining and FSW, process monitoring can serve as the basis for reducing chaotic tool

behavior and, thereby, provides a means for improving part quality in FSW as it has in machining.

In FSW, the tool tends to oscillate side-to-side (nominally transverse to applied loading vector) while under the local dynamic side loading conditions imposed on the tool at the tool-workpiece interface [4]. In machining, when the tool oscillates in a chaotic manner, a self-excited vibration phenomenon called “chatter” tends to form, leaving erratic markings on the newly cut surface. Similar chaotic oscillations in FSW tend to be associated with the formation of volumetric defects (voids) within the joint, resulting from the lack of consistency in the reconsolidation of material along the joint line [6].

The advancing, rotating FSW tool presses against the material directly ahead of it, creating a shearing action that extends around the tool front. In a generalized manner, when the material directly in front of the tool is sufficiently heated under the pressure and shearing action imposed on it by the advancing, rotating FSW tool, thin layers of material are transported from the advancing side of the tool to the retreating side of the tool. This action is repeated as the material ahead of the tool is again heated and pressed against sufficiently to cause it to shear and be transported along the front of the advancing tool. Each time material is transported across the face of the tool, cooler material is again exposed to the leading face of the tool.

This sequence of events leads to a repeating process of heating and shearing followed by heating and shearing (heat – shear – heat – shear ...). The new interface ahead of the tool is again pressed upon until it is sufficiently heated to move the next band of material along the tool front from the advancing side to the retreating side. This undulation in metal movement along the leading edge of the tool promotes an oscillatory or alternating pattern in both normal and shear forces acting on the tool surface, which in turn causes the tool to move in a periodic or oscillatory motion, nominally side-to-side, as the tool is advanced. This process is schematically depicted in Figure 1.

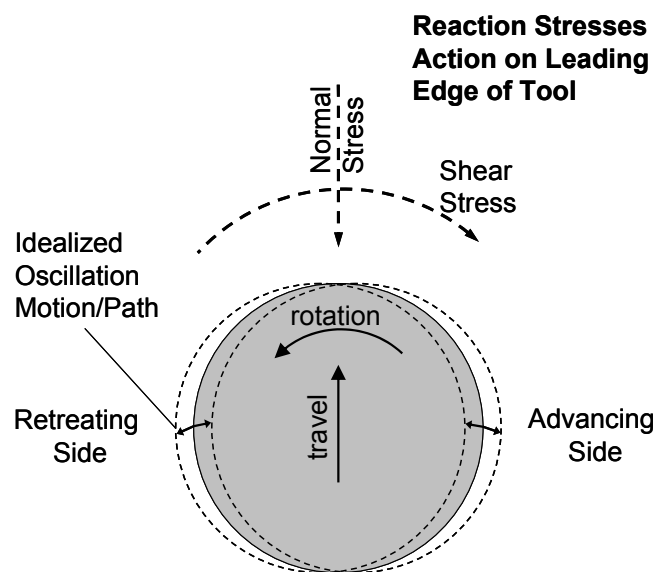


Figure 1: Schematic swept volume cross-section of a generic FSW tool probe located midway below the tool shoulder and the end of the probe [4].

The schematic in Figure 1 depicts the idealized oscillation of a mid-plane cross-section of a weld tool as it advances. Tool rotation is counter-clockwise and the direction of travel is toward the top of the page. The reaction forces act on the tool in opposition to the tool motion. A periodic shearing and movement of metal along the leading edge of the tool – from the advancing side to the retreating side – results and the tool oscillates side-to-side (nominally) in response to the dynamic reaction forces acting on the leading edge of the FSW tool probe.

Material flow and the associated resultant forces acting upon the tool are actually much more complex than idealized in the model shown in Figure 1. With the tool probe completely submerged in the work-piece, forces act on the probe from multiple directions in response to its dynamic loading environment, the resultant of which may be measured experimentally [6]. The full engagement of the rotating, advancing FSW tool further aggravates its tendency to oscillate in a chaotic manner. Adding to the complexity of FSW tool oscillatory motion is the spinning motion of the tool shoulder face on the surface of the work-piece. This tends to cause a wandering or walking motion of the end of the tool, which even further promotes chaotic tool behavior as the tool seeks (or seeks to establish) a center of rotation on the work-piece surface.

Uniformity in FSW tool oscillations is dependent upon the periodicity (or lack thereof) in the material flow behavior around the tool front. It is anticipated that the lower the abruptness in the material heating and shearing cycle, the less likely the process will become chaotic in its behavior (action). Selection of tool features and process parameters are expected to contribute to the overall stability of the tool control process.

The two e-NDE algorithms evaluated earlier for Friction Stir Welding (FSW) [3] were previously developed by Boldsaikhan et al. [5]. The first e-NDE algorithm is based on neural network and discrete Fourier transform techniques, and the second e-NDE algorithm uses phase-space approaches. Since the two algorithms produce a binary output (either flaw-detected or flaw-not-detected), Probability of Detection (POD) analyses were performed to assess the flaw-detection performances of the e-NDE methods as compared with the conventional NDE techniques: X-ray and ultrasonic phased-array (UPA) [3]. The actual volumetric defect sizes were measured from the macro cross-sections of the joints prepared from the systematically-chosen locations along the joint length (Figure 2). According to the POD analysis, which is based on the maximum-likelihood method of detection, the neural network-based algorithm provided significantly better detection performances compared to the conventional ultrasonic and X-Ray test results [3, 4]. In fact, the e-NDE methods outperformed the conventional NDE techniques by predicting the emergence of volumetric defects before they became detectable by macrographic examination through detecting irregularities in material flow (shown schematically in Figure 3).

The inspection results for one round-robin plate in particular (CFSP08502-1) provided a clear illustration of the capability of the e-NDE technique to detect the emergence of voids before they grow to sizes detectable by standard NDE and destructive testing techniques. According to the findings included in the NDE inspection reports, a volumetric indication identified near the end of the weldment was found by the different participants in the round-robin test program to begin at differing positions and to extend to varying lengths. The different findings for the location

and extent of the indication are marked within the red box in Figure 2. The mark for the e-NDE finding – which occurs sooner and extends further along the length of the weld than do the NDE location markings – is located on the plate just to the right of the red box included in Figure 2.

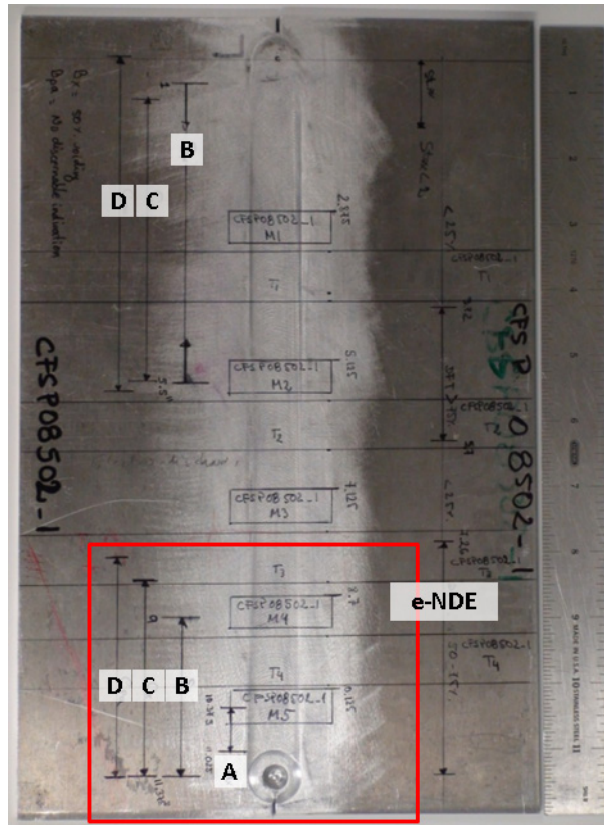


Figure 2: Plate CFSP08502-01 marked with the different NDE inspections results [3]. The area outlined by the red box is featured in Figure 3.

Careful examination of Figure 2 reveals plate separation near the exit hole. It is believed that the void initiated and grew due to this plate separation at the end of the weld. A gap between two butting workpieces can become an issue in production of friction-stir-joined structures. It can be caused by a deficiency in mechanical fixturing, the distortion induced by the welding process, or simply uneven faying surfaces of the two butting workpieces.

Figure 3 features the area of the test plate outlined by red in Figure 2. Included in Figure 3 is a series of macrographs taken of samples excised from the region in which the indication of a forming void at the end of the weld was first detected (with respect to the direction of travel). Each section was excised transverse to the joint line and evaluated to document the presence (or absence) and size of voids in this region. Two micrographs are included in Figure 3 to show the presence of the voids emerging in the last of the series of macrographs.

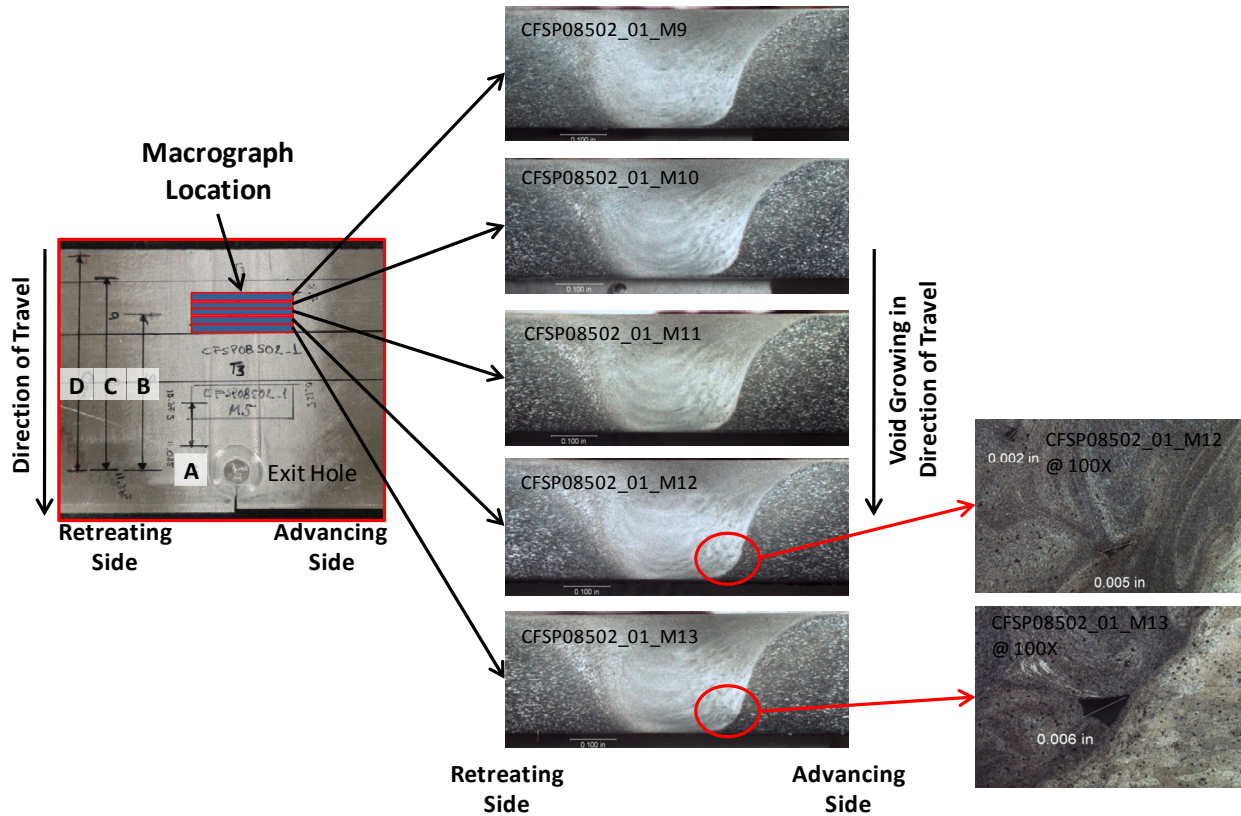


Figure 3: Macro-sections taken from coupon CFSP08502-01 which show the emergence of a void along the direction of welding [3]. The location of this section of the weldment is indicated by the red box in Figure 2.

A schematic showing the differences in detection of the start and extent of the indication associated with the weld in this plate is provided in Figure 4. The early void formation stage was first detected by the e-NDE technique (Figure 2), followed by the inspections represented by D, then C, B, and A in that order.

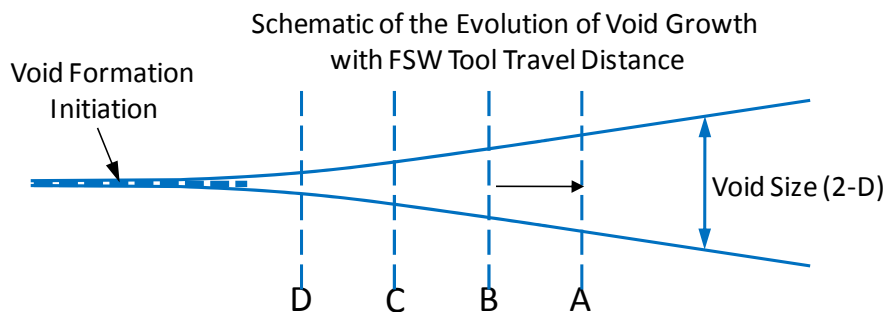


Figure 4: Schematic of evolution of void growth with FSW tool travel distance from the end of the plate [3].

As discussed in the previous section, the e-NDE technique relies on the presence of chaotic tool behavior to detect void formation. Thus, long before the volumetric defect actually emerged, as

evidenced by the e-NDE results, chaotic behavior in the Y-feedback force signal was beginning to increase as the weld progressed to the end of the plate (perhaps related to insufficient clamping coupled with end-of-the-plate effects). This growing chaotic behavior corresponded to an increasing lack of consolidation of the joint material, i.e. void formation.

In summary, this series of cross-sectional macrographs presented in Figure 3 shows that the e-NDE method is capable of predicting the emergence of volumetric defects even before voids open up during the welding process. This capability conceivably provides the time necessary to correct the FSW process through process parameter adjustments. The potential for this approach to be realized has been confirmed by the correlation of the macrographic inspection of void growth along the direction of tool travel with feedback force behavior. Based on the findings of this study, then, it is anticipated that the e-NDE technique can be transformed into a dynamic method for controlling FSW as a self-governing and self-correcting process capable of producing void-free joints.

Experimental Approach

Early detection of gaps between two butting workpieces is crucial for in-process monitoring, so that a preventive action can be carried out before the weld gets detrimental. The gap may introduce surface-lack-of-fill defects, subsurface voids, root flow imperfections, and excessive flashes that reduce the joint area. In this study, a neural-network-based e-NDE method developed by Boldsaikhan et al. [5] and tested by Gimenez Britos et al. [3] was used. In the present study e-NDE was used to detect the early formation of volumetric defects caused by the gaps with rectangular and diamond shapes. The ultimate goal of this research is to fold: 1) demonstrate that the force feedback signals measured from the weld tool can provide early indications of volumetric defects; and 2) that an e-NDE technique can be used for detecting those indications. This observation is important since, as shown in the earlier studies [3, 4], the conventional non-destructive techniques tested were not able to capture early indications of volumetric defects.

Aluminum AA2024-T351 plate material 6.35 mm (0.25 inch) thick and the weld tool shown in Figure 5 were selected for this study based on the prior research [3, 4]. The weld tool had a 20 mm (0.8 inch) diameter shoulder with the Wiper™ feature [10], and a threaded twisted-flat probe with the 10-degree taper angle. The dimensions of each plate are 51 mm (2 inches) wide, 305 mm (12 inches) long, and 6.35 mm (0.25 inch) thick. Two AA2024-T351 plates were then butted together to form the selected gap geometry and size. The joining surfaces of the two plates were machined to have gaps with four different geometries including full and half diamonds, and full and half rectangles, as illustrated in Figure 6. The longitudinal center of the gaps coincides with the longitudinal center of the joint line between the two butting plates. The length of a gap machined into each individual plate was 51 mm (2 inches), and the cut depth was 1.6 mm (0.063 inches). For single-sided gaps, the cut was always placed on the advancing side of the weld.

Wiper™



Figure 5: Weld tool with the Wiper™ shoulder [10, 11].

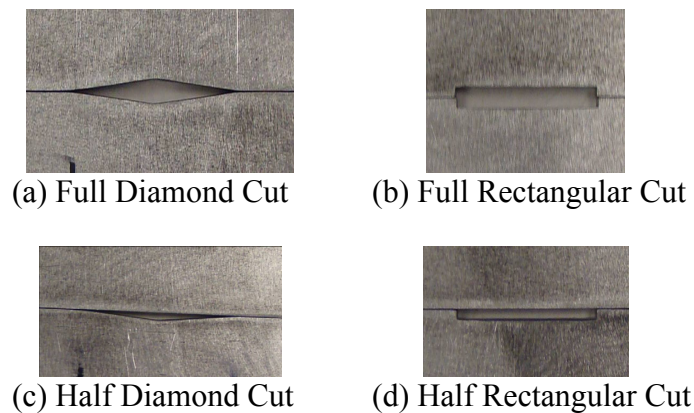


Figure 6: Gaps with the shapes of full diamond (a), full rectangle (b), half diamond (c), and half rectangle (d). The cut depth into the plate is 1.6 mm (0.063 inch).

Prior to welding, the plates were orbital-sanded and then wiped with methyl-ethyl-ketone (MEK). All welds were made with a spindle speed of 400 rotations/minute (rpm), a travel speed of 330 mm/minute (13 inches/minute), tool tilt angle of 0.5 degree, and the axial load of 29.6 kN (6659 pound-force, lbf). These process parameters were selected based on the prior work, which showed that this set of parameters produced fully consolidated joints [3, 4]. All the welds were made under the axial load control mode in which the Z-load is regulated to a commanded value. The length of each friction stir joint was about 254 mm (10 inches). All FSW was conducted on a MTS® ISTIR™ PDS FSW machine located in the Advanced Joining and Processing Lab (AJP) of the National Institute for Aviation Research (NIAR) at Wichita State University.

Two friction stir joints were made for each gap geometry and size in order to perform both metallographic and tensile examinations. A cut plan for the metallographic examination is depicted in Figure 7, and a cut plan for the tensile examination is shown in Figure 8. To observe the metallographic evolution of each weld, twenty cross-sectional macros were generated from the vicinity of the gap, where the spacing between two adjacent cuts was 6.35 mm (0.25 inch) (Figure 7). Correspondingly, to observe the tensile strength variation in each weld, five tensile coupons were sampled from the vicinity of the gap, where the width of each coupon was 19 mm (0.75 inch) as given in Figure 8.

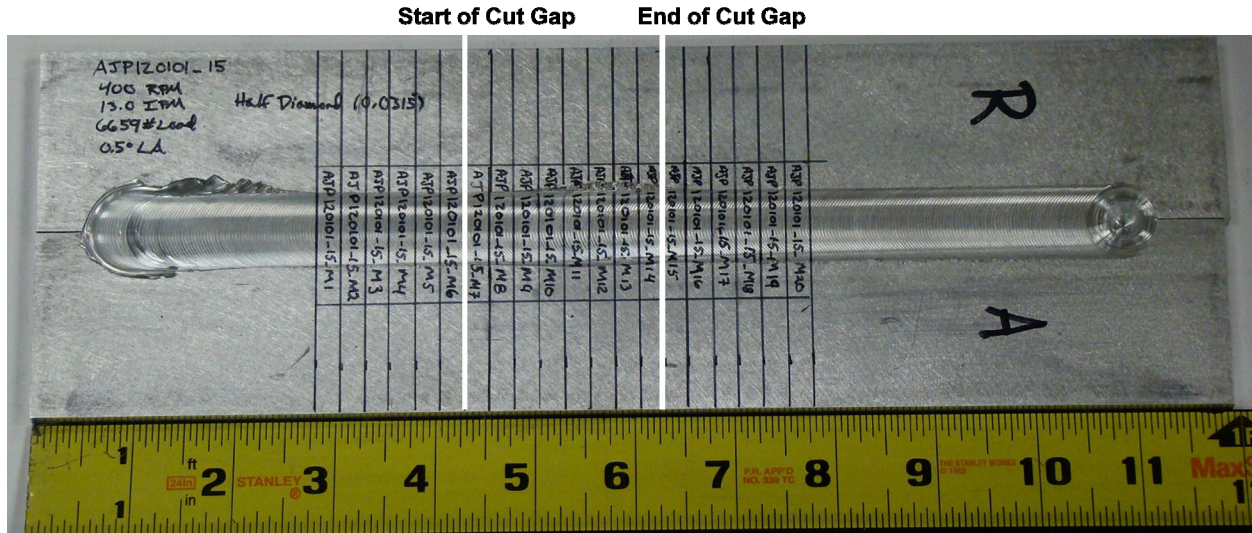


Figure 7: Cut plan for cross-sectional macros.

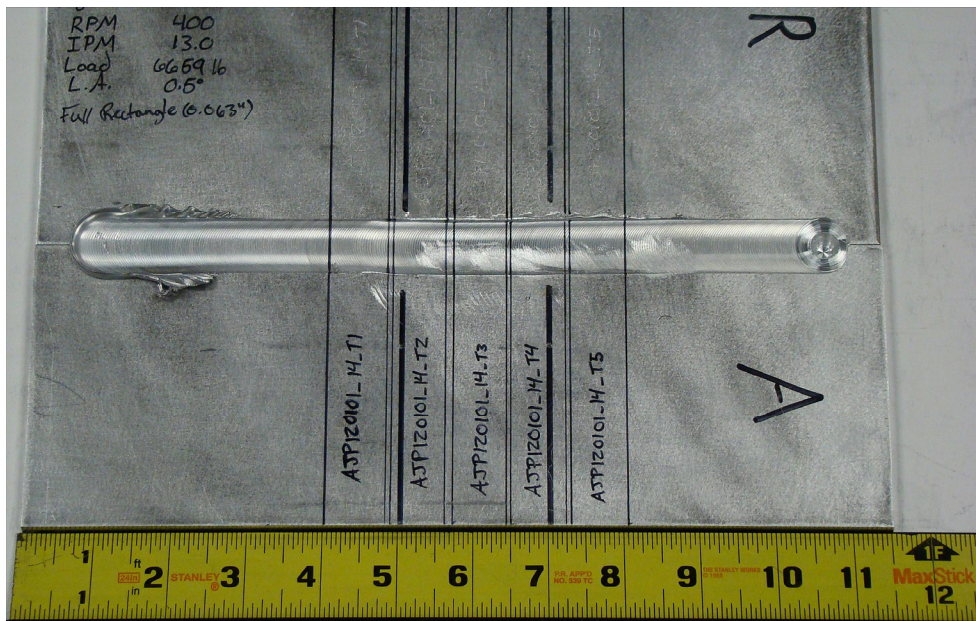


Figure 8: Cut plan for tensile coupons.

The gap is located between 127 mm (5 inches) and 178 mm (7 inches) from the left end of the plate.

The FSW machine is equipped with force sensors installed in the weld head assembly. It is also equipped with a data acquisition system capable of simultaneously capturing more than 20 different signals at a sampling rate of up to 1000 Hz. The data acquisition system was configured to generate data files that include the following feedback signals:

- Travel Speed Feedback
- Spindle Speed Feedback
- Tool X, Y, Z Positions
- Tool X, Y, Z Forces

- Tool X, Y, Z Torques
- Roll, Pitch, Yaw Angles

In this study, the force feedback signals were collected at 512 Hz during each welding experiment and analyzed with a neural network model developed by Boldsaikhan, et al. [5].

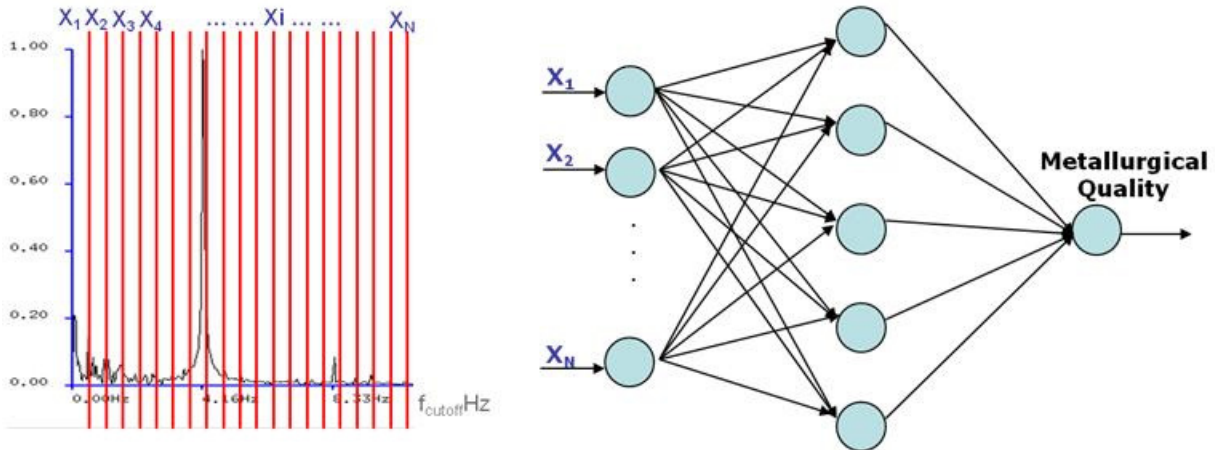


Figure 9: Feature extraction from frequency spectrum (left) and neural network architecture (right).

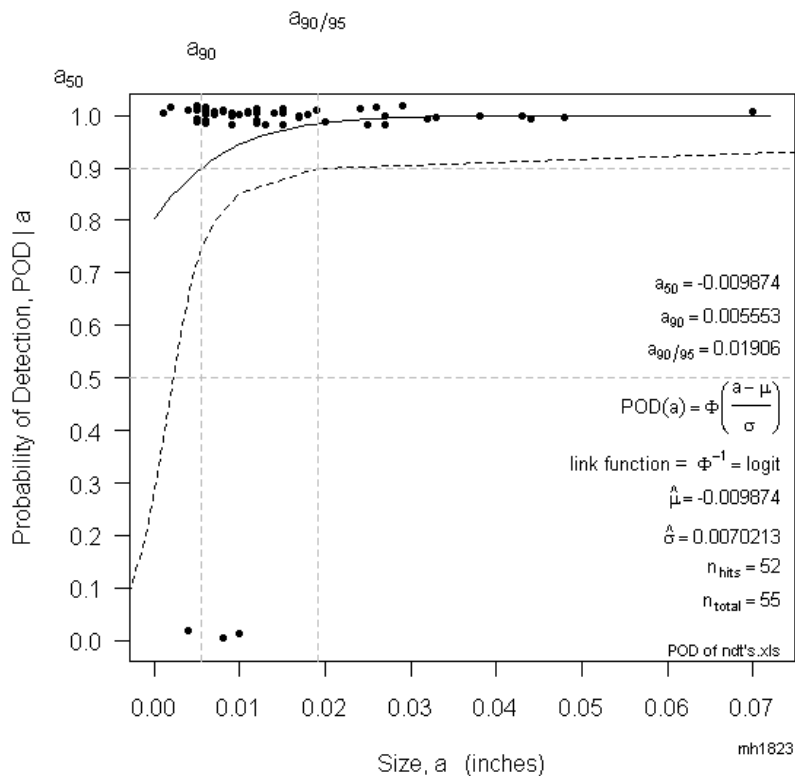


Figure 10: Mean probability of detection versus void size for the NN analysis results from [12].

Neural networks (NN) have an excellent capability for learning any nonlinear mapping from training examples and then generalizing what they have learned. Consequently, they can deal with unexpected novel input patterns. The NN model used in this study had one input layer, one hidden layer, and one output unit. Because this study is an extension of the research reported by Gimenez Britos [12], the NN model for this study was trained by the force feedback data generated by the earlier research.

For the time series signal analysis, this study implemented a sliding time-window approach in order to iteratively evaluate the entire time spectra of the tool X and Y forces. The length of the sliding time-window was 2 seconds and the step size of the window was 1 second. Frequency spectra of the weld tool X and Y forces were generated from the time-window using the discrete Fourier transform.

Input (feature) vectors to the NN model were extracted from the frequency spectra of the tool X and Y forces as illustrated in Figure 9. In Figure 9, the frequency spectrum of a feedback force is divided into N (integer number) bins, and the average of each bin is fed into the NN model, and the output unit of NN produces a binary value: 1 = “acceptable weld” and 0 = “unacceptable weld.” The probability of detection (POD) NN model was based upon a binary regression analysis and is shown in Figure 10. As reported by Gimenez Britos [12], the NN model identified voids with a length greater than 0.13 mm (0.005 in) at a 90% mean POD, and a length of 0.48 mm (0.019 in) with a 90% POD at a 95% confidence level (Figure 10).

Results and Discussion

The NN evaluation output results of the friction stir joints generated for the different gaps studied are plotted in Figures 11, 13, 15, and 17. Correspondingly, metallographic evolutions of the friction stir joints are illustrated in Figures 12, 14, 16, and 18, respectively. As shown in the figures containing the NN evaluation outputs, the NN model successfully identified not only the gap locations but also the locations of flashes generated in the beginning of the weld as well as in the gap region. The occurrence of flash (loss of material from under the weld tool shoulder) in the gap region was induced by the excessive plunge depth of the weld tool under the force control mode in order to recover the missing pressure caused by the gap.

The evidence of the plunge depth variation is provided in Figure 19. In Figure 19, when the leading shoulder encounters the gap edge, the plunge rate becomes faster as the gap shape is more pronounced. Both gaps and the occurrence of flash introduce heterogeneous (imbalanced or non-uniform) radial pressure on the tool surfaces that cause instability in the tool feedback forces. They also generate a reduced joint area (cross-section) between the two workpieces, which makes the joint region weaker. Therefore, the NN model was successfully used to classify weld sections with gaps and/or flash as acceptable or unacceptable based on the indications in the force feedbacks. Note that although the half diamond gap was completely healed up after welding (Figure 11), the NN model classified the weld as unacceptable since it produced a significant amount of flash.

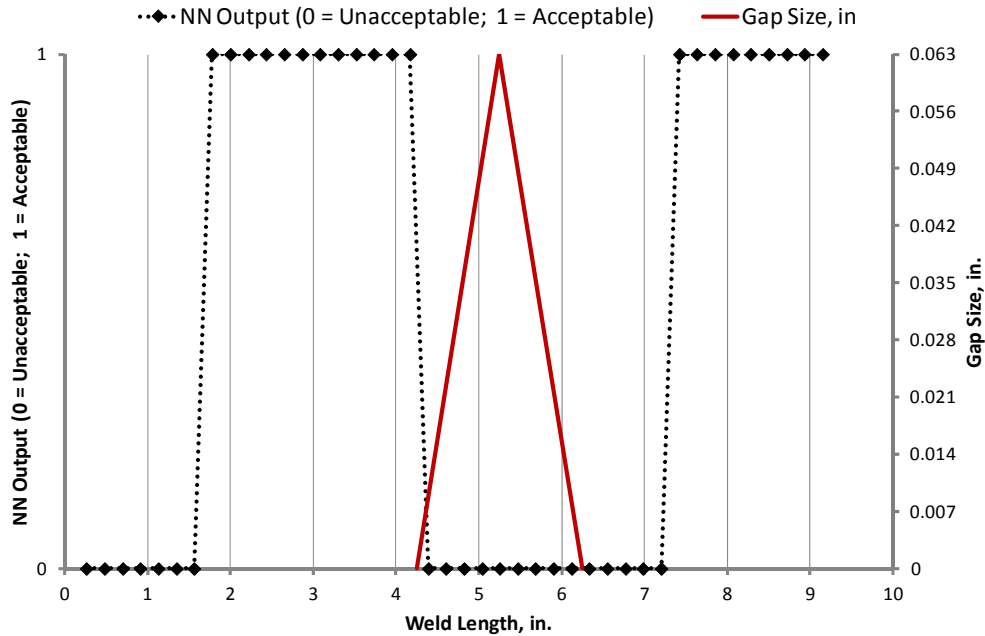


Figure 11: NN detection of 1.6 mm (0.063 inch) wide half diamond gap. Each NN output point refers to the tool center point that advances over the weld length.

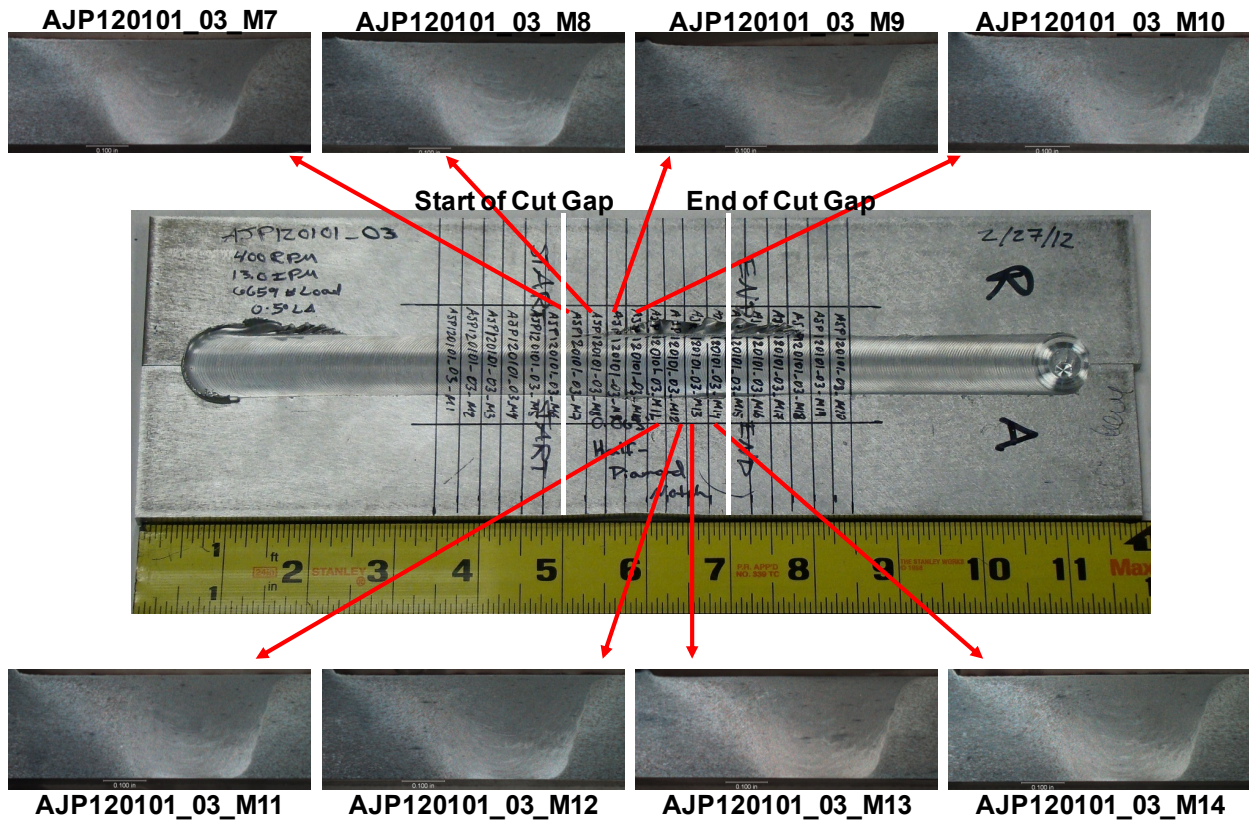


Figure 12: Cross-sectional macrographs associated with 1.6 mm (0.063 inch) wide half diamond gap. The half diamond gap was machined into the advancing side plate (bottom plate).

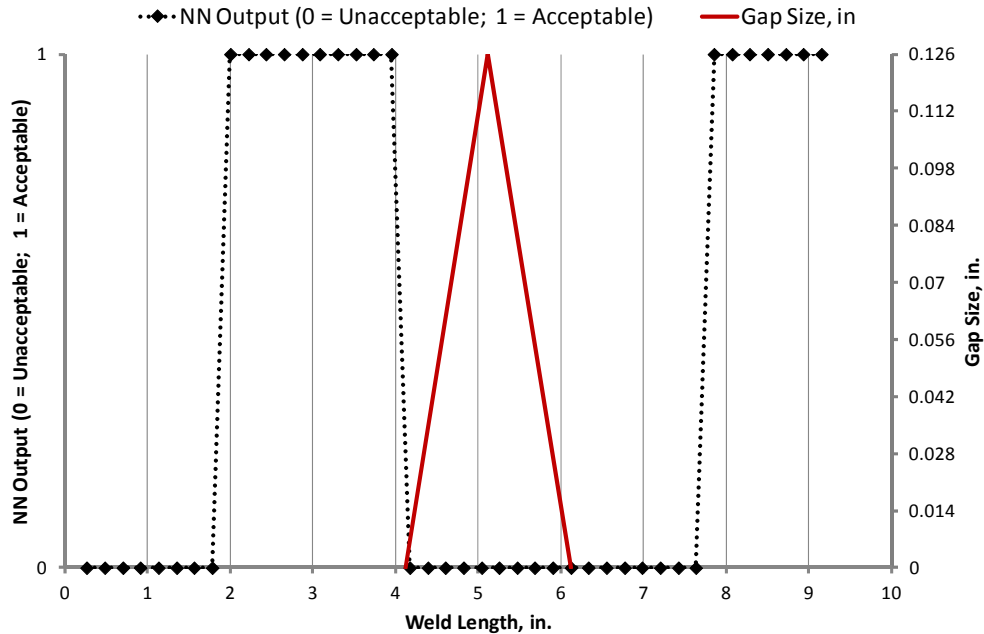


Figure 13: NN detection of 3.25 mm (0.128 inch) wide full diamond gap. Each NN output point refers to the tool center point that advances over the weld length.

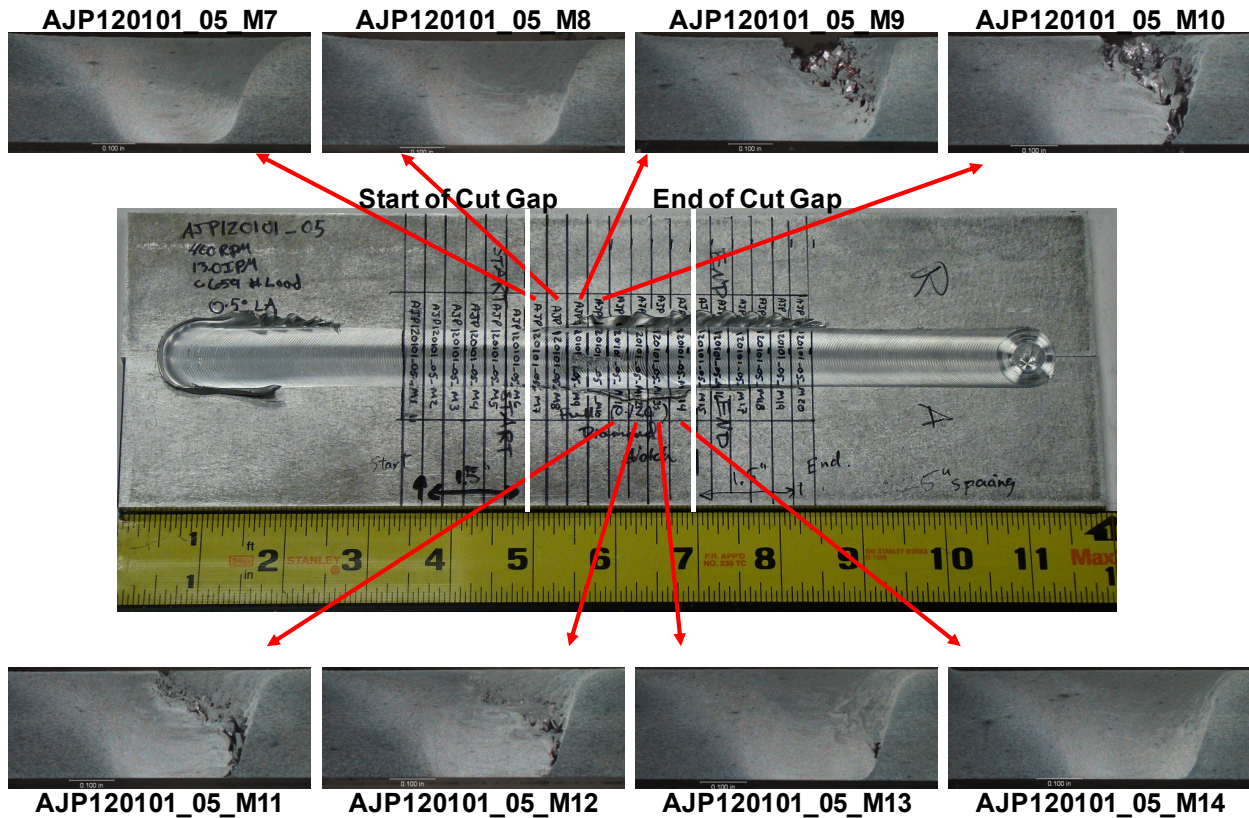


Figure 14: Cross-sectional macrographs associated with 3.25 mm (0.128 inch) wide full diamond gap. Both-side plates were symmetrically machined to form the full diamond gap.

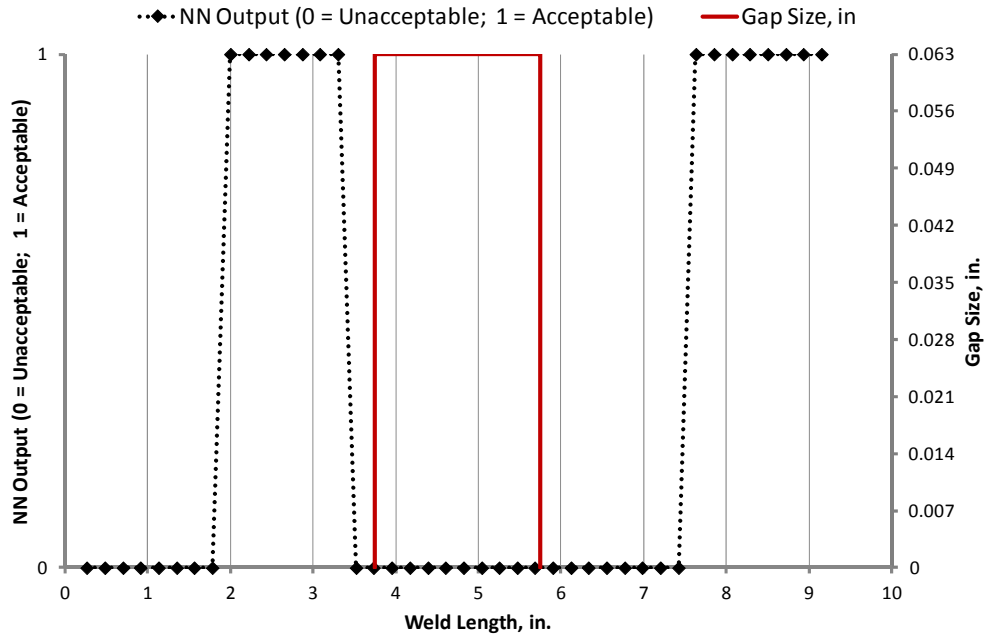


Figure 15: NN detection of 1.6 mm (0.063 inch) wide half rectangular gap. Each NN output point refers to the tool center point that advances over the weld length.

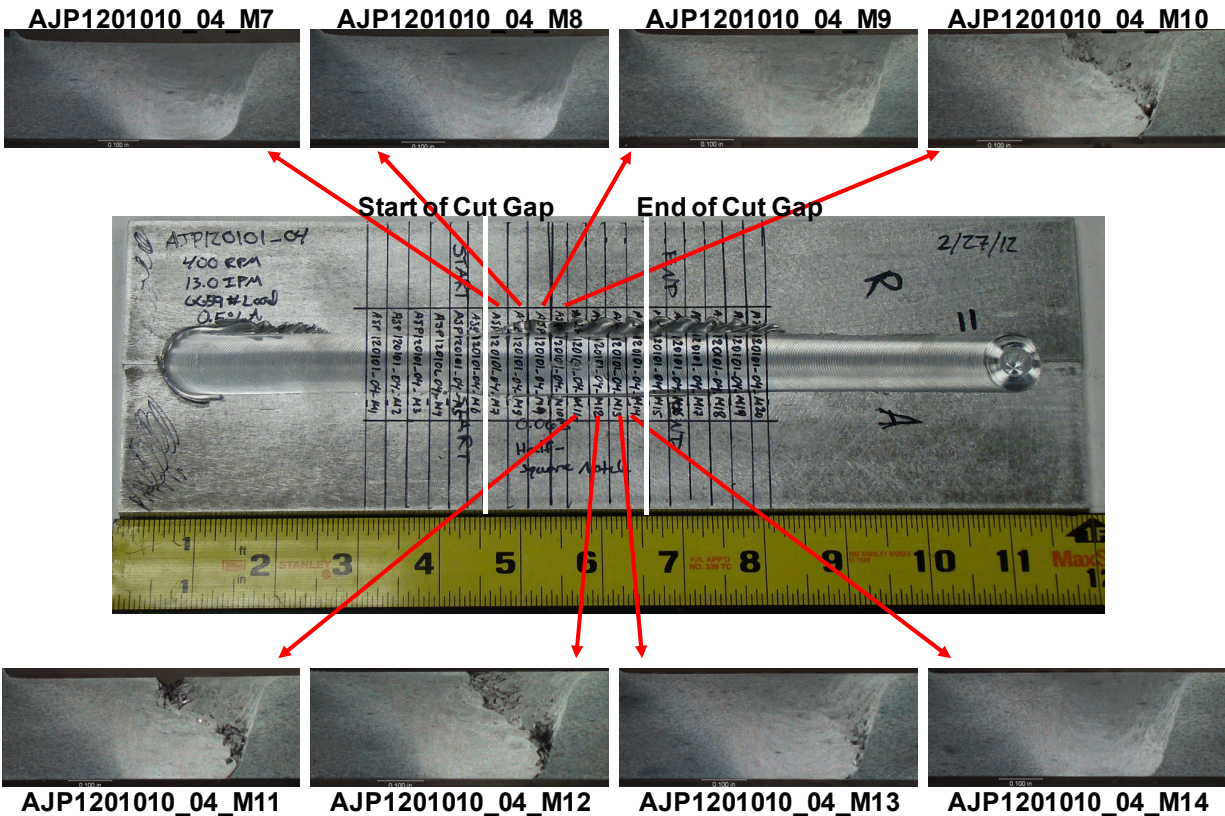


Figure 16: Cross-sectional macrographs associated with 1.6 mm (0.063 inch) wide half rectangular gap. The half rectangular gap was machined into the advancing side plate (bottom plate).

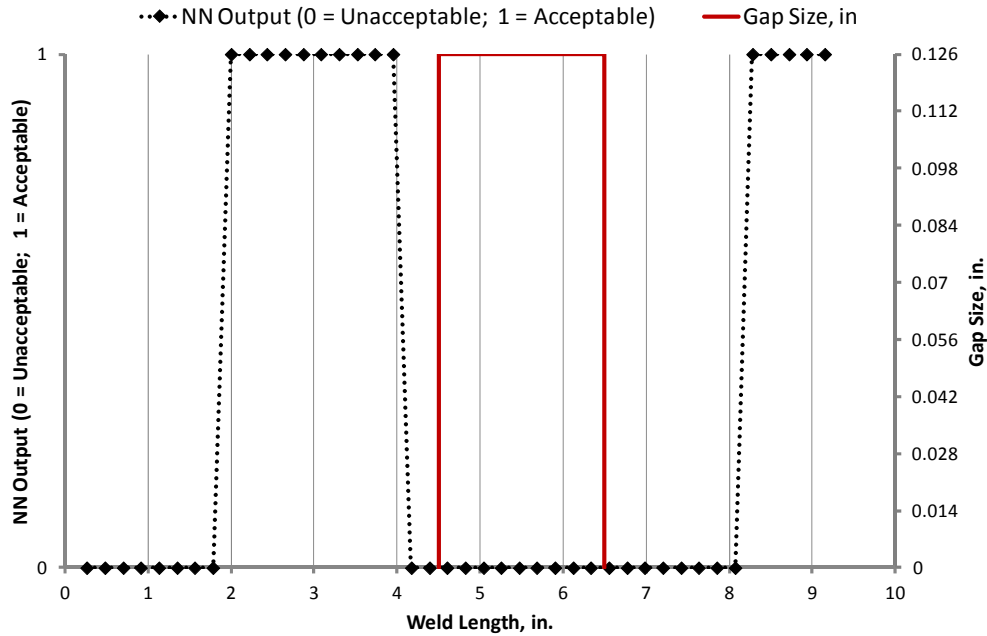


Figure 17: NN detection of 3.25 mm (0.128 inch) wide full rectangular gap. Each NN output point refers to the tool center point that advances over the weld length.

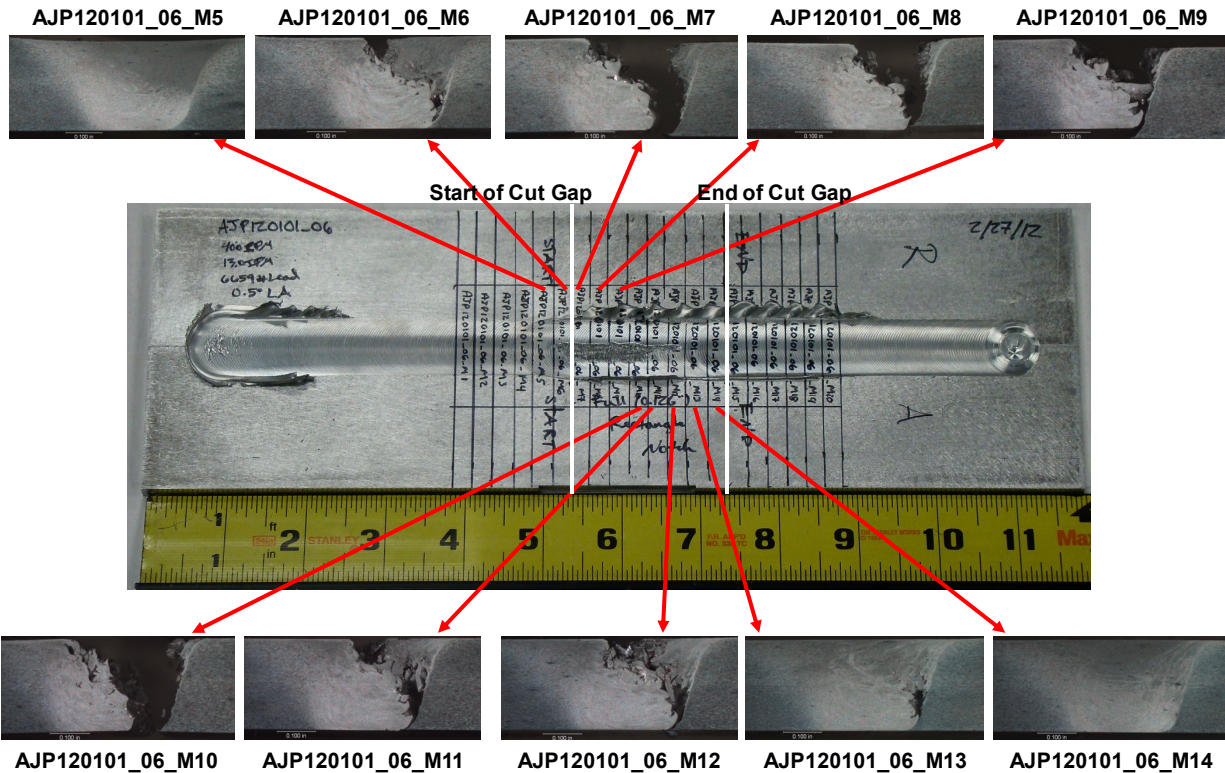


Figure 18: Cross-sectional macrographs associated with 3.25 mm (0.128 inch) wide full rectangular gap. Both-side plates were symmetrically machined to form the full rectangular gap.

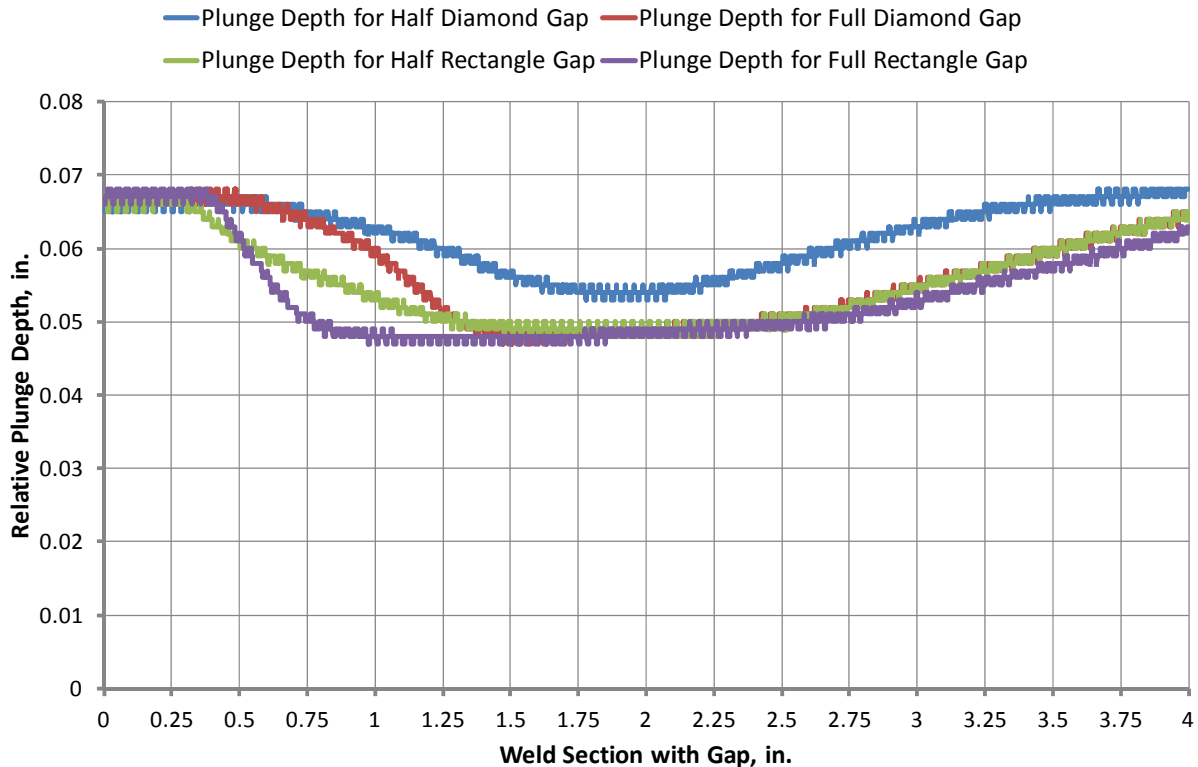


Figure 19: Relative plunge depth versus weld section with gap.
Each gap exists between 19 mm (0.75 in.) and 69.9 mm (2.75 in.) within the weld length.

The NN model detected the rectangular gaps earlier than the diamond gaps as observed in Figure 11, Figure 13, Figure 15, and Figure 17. The tensile coupons sampled from the half-diamond-gap section demonstrated the same strength as the coupons sampled from the gapless weld section. The average tensile strength was 433 MPa (62.8 ksi) with the 5.5 MPa (0.8 ksi) variation. The tensile coupons associated with the full diamond gap and the half and full rectangular gaps failed at very low load levels, below 414 MPa (60 ksi) in the nugget area, due to defects caused by a lack of consolidation in the region of the pre-existing gaps.

Conclusions

The emergence of voids caused by the presence of preexisting gaps along the joint line was readily detected with e-NDE. Coupons with both triangular and rectangular gaps prepared from AA2024-T3 plate stock were tested. Rectangular gaps were detected earlier than the diamond gaps due to the abrupt versus the gradual encounter of the tool with the gap. The e-NDE NN model was successfully used to determine the onset of void formation, when present, and to classify sections of the welds with gaps and/or flash as acceptable or unacceptable based on the indications in the force feedbacks. The discriminating capability of the technique was also tested. Although a half diamond gap was completely healed up after welding, the NN model classified the weld as unacceptable since it produced a significant amount of flash.

The implementation of the e-NDE approach transforms FSW into a GREEN² (“green squared”) welding technology. Taken alone, FSW is a green manufacturing process in comparison to conventional fusion welding techniques, which produce toxic gases and radiation emissions. With the application of e-NDE as a real-time quality monitoring process, the level of “greenness” to the overall FSW process is multiplied through reducing costly post-weld inspection procedures that potentially involve toxic chemicals or emissions. Furthermore, the development of e-NDE methods provides the most important step towards creating an intelligent algorithm for a process control system for achieving the highest quality friction stir welded joints.

Acknowledgements

Funding for this research was made available through the Wichita State University (WSU) Research Site of the Center for Friction Stir Processing (CFSP), a National Science Foundation (NSF) Industry / University Collaborative Research Center (IUCRC). The authors would especially like to thank Raeann Edson and Christian Walden for welding, preparing, and testing the test coupons. The authors would also like to thank the Site members active at the time this research work was completed, including Bombardier, Gulfstream, Hawker Beechcraft, and Space Exploration Technologies Corporation.

References

- [1] D. A. Burford, "Friction Stir Welding of Airframe Structure: From One Delivery System to Another," *SAE 2003 Transactions, Journal of Aerospace*, vol. 112, no. Section 1, pp. 295-300.
- [2] C. A. Widerner, B. M. Tweedy and D. A. Burford, "Effect of Fit-up Tolerances on the Strength of Friction Stir Welds," in *47th AIAA/ASME/ASCE/AHS/ASC Structures, Structural Dynamics, and Materials Conference*, Newport, Rhode Island, 2006.
- [3] P. Gimenez-Britos, C. Widener, E. Boldsai Khan and D. Burford, "Probability of Detection Analysis of NDT Methods for Friction Stir Welded Panels," in *8th International Friction Stir Welding Symposium*, Timmendorfen Strand, Germany, 18-20 May 2010.
- [4] D. A. Burford, P. Gimenez Britos, E. Boldsai Khan and J. Brown, "Evaluation of Friction Stir Weld Process and Properties for Aerospace Application: e-NDE for Friction Stir Processes," vol. 6th Annual Technical Review Meeting, 19 May 2010.
- [5] E. Boldsai Khan, A. Logar and E. Corwin, *Real-Time Monitoring in Friction Stir Welding: The Use of Feedback Forces for Nondestructive Evaluation of Friction Stir Welding*, Lambert Academic Publishing, 2010.
- [6] E. Boldsai Khan and D. Burford, "Generalized e-NDE Algorithm for Friction Stir Welding," in *9th International Friction Stir Welding Symposium*, The Von Braun Center, Huntsville, AL, May 15-17, 2012.
- [7] Y. Zhang and N. Sims, "Milling workpiece chatter avoidance using piezoelectric active damping: a feasibility study," *Smart Mater. Struct.*, vol. 14, p. N65–N70, 2005.
- [8] W. Arbogast, "Modeling Friction Stir Joining as a Metalworking Process," in *Hot Deformation of Aluminum Alloys III*, 2003.
- [9] T. Jene, G. Dobmann, G. Wagner and D. Eifler, MonStir – Monitoring of the Friction Stir

9th International Friction Stir Welding Symposium
The Von Braun Center, Huntsville, AL. 15-17 May 2012

Welding Process, 7th International Symposium on Friction Stir Welding ed., Awaji Island, Japan, 20-22 May 2008.

- [10] D. A. Burford, "Friction stir welding tool having a scroll-free concentric region," Patent Patent No. 8,016,179.
- [11] D. A. Burford, B. M. Tweedy and C. A. Widener, "Influence of Shoulder Configuration and Geometric Features on FSW Track Properties (Paper 36)," in *Proceedings of the 6th International Friction Stir Welding Symposium*, Saint-Sauveur, Nr Montreal, Canada, 2006.
- [12] P. Gimenez Britos, *Probability of Detection in Friction Stir Welding Using Nondestructive Evaluation Techniques*, Masters Thesis, Industrial Engineering, Wichita State University, May 2010.